

Article

# Sulfonated Hydrothermal Carbons from Cellulose and Glucose as Catalysts for Glycerol Ketalization

Pablo Fernández <sup>1</sup>, José M. Fraile <sup>2,\*</sup> , Enrique García-Bordejé <sup>3</sup>  and Elisabet Pires <sup>1,2,\*</sup> 

<sup>1</sup> Dpto. Química Orgánica, Facultad de Ciencias, Universidad de Zaragoza, E-50009 Zaragoza, Spain; pablozgz@hotmail.com

<sup>2</sup> Instituto de Síntesis Química y Catálisis Homogénea (ISQCH), Facultad de Ciencias, C.S.I.C. - Universidad de Zaragoza, E-50009 Zaragoza, Spain

<sup>3</sup> Instituto de Carboquímica (ICB-CSIC), Miguel Luesma Castán 4, E-50018 Zaragoza, Spain; jegarcia@icb.csic.es

\* Correspondence: jmfraile@unizar.es (J.M.F.); epires@unizar.es (E.P.); Tel.: +34-976-553-514 (J.M.F.); +34-976-553-501 (E.P.)

Received: 1 July 2019; Accepted: 23 September 2019; Published: 25 September 2019



**Abstract:** Solketal is one of the most used glycerol-derived solvents. Its production via heterogeneous catalysis is crucial for avoiding important product losses typically found in the aqueous work-up in homogeneous catalysis. In this work, we present a study of the catalytic synthesis of solketal using sulfonated hydrothermal carbons (SHTC). They were prepared from glucose and cellulose resulting in different textural properties depending on the hydrothermal treatment conditions. The sulfonated hydrothermal carbons were also coated on a graphite microfiber felt (SHTC@GF). Thus, up to nine different solids were tested, and their activity was compared with commercial acidic resins. The solids presented very different catalytic activity, which did not correlate with their physical-chemical properties indicating that other aspects likely influence the transport of reactants and products to the catalytic surface. Additionally, the SHTC prepared from cellulose showed better reusability in batch reaction tests. This work also presents the first results for the production of solketal in a flow reactor, which opens the way to the use of SHTC@GF for this kind of reactions.

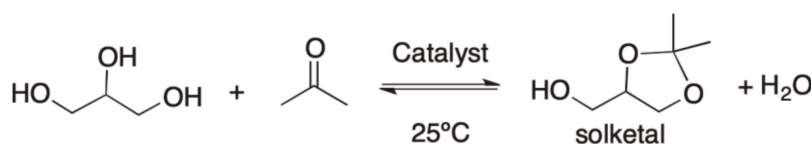
**Keywords:** sulfonated hydrothermal carbon; solketal; sulfonic solids; ketalization; continuous flow

## 1. Introduction

Lignocellulosic biomass is a renewable and accessible feedstock for the production of commodity chemicals and fuels [1]. The main component of raw biomass is cellulose, a biopolymer made from glucose monomers. The hydrothermal treatment of cellulose was first developed to hydrolyze cellulose into liquid fuels or platform chemical molecules such as furfurals [2–5]. The treatment under pressure of cellulose in water, at temperatures in the 150–400 °C range, gives rise to a mixture of soluble organic substances and a carbon-rich solid product, whose relative amount depends on the conditions. Only until recently, attention has been paid to the solids resulting from hydrothermal treatment [6–8]. It is widely reported that the hydrothermal treatment of saccharides such as glucose produces carbon microspheres of uniform sizes under very mild process conditions [9–12]. Compared to glucose, cellulose is a more convenient feedstock because it is more abundant and inexpensive and studies can be found in the literature on the hydrothermal carbonization of cellulose [13–16]. Sulfonated hydrothermal carbons derived from renewable raw materials are envisaged as sustainable catalysts and are often applied in biomass transformations [17]. However, the hydrothermal carbons prepared from cellulose have been rarely used as catalyst precursors.

Together with the use of renewable raw materials, the use of green solvents is a trending topic in biorefineries. Among the different alternatives, the use of glycerol itself and its derivatives as renewable

solvents has attracted great attention in the last decade [18] and, in particular, glycerol carbonate [19] and solketal [20] can be considered the most applied glycerol derived solvents up to now. In order to envisage the possibility of producing large amounts of solketal (Scheme 1), a sustainable synthetic methodology must be developed and, thus, many works have been published so far related to the study of different catalytic systems for the reaction of glycerol with acetone [21]. One of such examples is the use of homogeneous acid catalysts, which implies an aqueous work-up of the reaction. Due to the large transfer of the ketal to the aqueous phase, the global isolated ketal yield is seriously lowered, up to 70% [22]. Thus, many efforts have been devoted to the search of efficient heterogeneous catalysts for this reaction. Among the different catalytic systems, heterogeneous Brønsted acids, such as the sulfonic resin Amberlyst 36 [23], sulfonic-functionalized SBA-15 [24] or mesoporous zeolites [25], and heterogeneous Lewis acids, such as Zr- and Hf-TUD-1 and Sn-MCM-41 [26], have been described as effective catalysts for solketal production. In the case of zeolites, the surface area and the presence of mesoporosity seems to also play a crucial role for obtaining high glycerol conversions (80%) and total solketal selectivity. In a recent work, glycidol has been described as starting material for solketal production and several heterogeneous catalysts were tried such as Nafion®NR50, supported metal triflates, K10 montmorillonite, and Amberlyst 15 [27]. In this case, Nafion®NR50 is described as the best catalyst, although high acetone/glycidol ratios and longer reaction times were needed in order to obtain high glycidol conversions.



**Scheme 1.** Overall reaction for the production of solketal.

It is also worth mentioning that in all the cases, reaction temperatures in between 343–353 K are used in order to achieve good solketal yields.

An interesting point when developing sustainable processes is the possibility of using heterogeneous catalysts that are also derived from renewable raw materials. As mentioned above, this is the case of carbons. Thus, sulfonated activated carbons obtained from olive stones [28] and hydrothermal carbons prepared from glycerine as biodiesel waste [29] have been proposed as catalysts in the reaction of glycerol and acetone. In both cases, the reaction proceeded smoothly at room temperature using 3 wt% catalyst. Conversions of glycerol of 80% and solketal selectivity over 95% were described.

Continuing the efforts we have done in our laboratory to develop low-cost and versatile biomass derived catalysts, in this work, sulfonated hydrothermal carbons were selected because of their renewable origin, mild preparation conditions and good catalytic performance shown in other acid-catalyzed reactions. More specifically, we present here for the first time the preparation and characterization of sulfonated hydrothermal carbons from cellulose, both bulk and deposited on graphite felt, as well as a comparative study of their activity with a previously described catalyst derived from glucose and commercial sulfonic resins, as acid catalysts in the synthesis of solketal, their reusability and the preliminary results in a flow reactor.

## 2. Results and Discussion

In previous works, we studied the synthesis of hydrothermal carbons from both glucose and cellulose [30–32]. Thus, the hydrothermal treatment of glucose leads to a carbon material (HTC) in the form of microspheres [30], with rather high density of oxygenated functional groups (oxygen/carbon molar ratio = 0.3) that confers to the solid a highly hydrophilic character. The surface area, determined by nitrogen adsorption, was very low (<10 m<sup>2</sup>/g) as well as the pore volume (0.014 cm<sup>3</sup>/g). However, the use of CO<sub>2</sub> as adsorbate indicated the presence of a larger surface area and pore volume

(>140 m<sup>2</sup>/g and 0.06 cm<sup>3</sup>/g, respectively), which is interpreted as an indication of the presence of ultramicropores (<0.7 nm) [31]. In agreement with the relatively high oxygen content, the different types of spectroscopic techniques, such as XPS (X-ray photoelectron spectroscopy) and CP-MAS-NMR (Cross Polarization-Magic Angle Spinning-NMR), indicated the presence of carbonyl and carboxylic groups, as well as furanic and benzofuranic (and probably phenolic) aromatic groups, together with a significant amount of aliphatic chains, associated with terminal or bridge groups between the aromatic rings [30]. The presence of such carboxylic groups confers a weak acidity (3.4 mmol/g, determined by back titration) to the HTC.

In the studies of hydrothermal carbonization of microcrystalline cellulose [32], different reaction conditions of temperature and time were tried, in the absence or in the presence of HCl at different concentrations to promote the partial hydrolysis of cellulose. The samples are named as Cel-temperature-HCl concentration (when used)-time, for example, Cel-195-20 h indicates an HTC prepared from cellulose at 195 °C for 20 h in the absence of HCl and Cel-215-2 M-40 h indicates a HTC prepared from cellulose at 215 °C, with 2 M HCl for 40 h. Analogously, the HTC from glucose is named as Glu-195-20 h, as in that case no HCl was used in the hydrothermal process. Although the hydrothermal carbons from cellulose showed similar general features to that prepared from glucose, the hydrothermal conditions (temperature, time, acid) significantly modified the morphology and textural properties of the HTC. Less developed microspheres, with oxygen contents ranging from 12.8 to 27.9% were obtained, together with surface areas measured with CO<sub>2</sub> from 104 to 386 m<sup>2</sup>/g. In fact, the surface area was used here to establish a sort of harshness scale of the hydrothermal conditions that we called “hydrothermal index” (H.I.) with an arbitrary scale of 0–20 [32]. The acidity of the cellulose derived HTCs, corresponding to carboxylic groups, determined by the difference between total acidity and the number of SO<sub>3</sub>H groups, also varied with the hydrothermal conditions, from 0.85 to 2.31 mmol/g, but it was always lower than the acidity of the HTC from glucose (3.42 mmol/g).

### 2.1. Synthesis and Characterization of Sulfonated Hydrothermal Carbon Catalysts from Cellulose

The HTC samples obtained from glucose and microcrystalline cellulose were sulfonated under the standard conditions, concentrated H<sub>2</sub>SO<sub>4</sub> at 150 °C for 15 h (see Materials and Methods). The sulfonated solid samples are named using the HTC precursor nomenclature followed by an S. That is, Cel-195-20 h-S indicates a sulfonated hydrothermal carbon (SHTC) prepared from cellulose at 195 °C in the absence of HCl for 20 h and subsequently sulfonated with H<sub>2</sub>SO<sub>4</sub>. Results of elemental analysis, textural properties and acidity of SHTC are collected in Table 1 together with the ones of the non-sulfonated samples for the sake of comparison.

As we previously reported [30], the sulfonation of Glu-195–20 h (sample 1 in Table 1) with concentrated sulfuric acid at 150 °C for >4 h preserves the morphology of microspheres, as well as the textural properties, with only an increase in CO<sub>2</sub> surface area and porosity (sample 1 vs. 1-S in Table 1). However, the sulfonation produces significant changes in the chemical composition. The sulfonated hydrothermal carbon (Glu-195-20 h-S, sample 1-S) is a more oxygenated carbon material, with an oxygen/carbon molar ratio around 0.5 and a sulfur content of 0.60–0.77 mmol/g, evenly distributed along the particles [31]. The number of total acid sites was larger than the amount of sulfonic sites, indicating that, besides sulfonation, the treatment with sulfuric acid produces additional reactions (mainly oxidations) on the HTC.

The sulfonated cellulose samples prepared in this work also suffered composition and textural changes upon sulfonation that will be now commented. As an example, Figure 1 gathers SEM (Scanning Electron Microscopy) images, CO<sub>2</sub> adsorption isotherm plots and pore volume distributions for two representative solids, Cel-195-2 M-20 h (sample 3, Table 1) and Cel-195-2 M-20 h-S (sample 3-S, Table 1). The plots for all the SHTC samples are gathered in the ESI. As it can be seen, changes in morphology are observed by SEM analysis, although some microspheres were still present upon sulfonation.

**Table 1.** Composition, textural properties and acidity of HTC and SHTC samples.

Id.	Sample	H.I.	wt%				S <sub>A</sub> (m <sup>2</sup> /g) <sup>a</sup>	V <sub>μP</sub> (cm <sup>3</sup> /g) <sup>b</sup>	SO <sub>3</sub> H <sup>c</sup>	T.A. <sup>d</sup>	COOH <sup>g</sup>
			C	H	O	S					
1	Glu-195-20 h <sup>e</sup>	0.0	66.3	4.4	29.9	–	143	0.057	–	3.42	3.42
1-S	Glu-195-20 h-S <sup>e</sup>	-	55.2	2.3	40.1	2.5	224	0.090	0.77	5.43	4.66
2	Cel-195-20 h <sup>f</sup>	2.4	68.3	4.5	27.1	–	201	0.083	–	2.31	2.31
2-S	Cel-195-20 h-S	-	53.3	2.8	40.5	3.4	272	0.099	1.07	4.45	3.38
2-S'	Cel-195-20 h-S-used	-	52.8	3.0	41.9	2.3	–	–	0.74	n.d.	–
3	Cel-195-2 M-20 h <sup>f</sup>	2.7	67.6	4.5	25.6	–	208	0.085	–	1.94	1.94
3-S	Cel-195-2 M-20 h-S	-	56.4	3.1	38.1	2.4	284	0.104	0.74	5.20	4.46
3-S'	Cel-195-2 M-20 h-S-used	-	58.0	3.2	37.0	1.8	–	–	0.58	n.d.	–
4	Cel-215-20 h <sup>f</sup>	3.2	70.0	4.5	25.3	–	220	0.092	–	2.09	2.09
4-S	Cel-215-20 h-S	-	52.6	3.5	40.9	3.0	226	0.083	0.96	3.34	2.38
5	Cel-195-5 M-20 h <sup>f</sup>	5.4	73.5	5.1	21.4	–	274	0.118	–	0.85	0.85
5-S	Cel-195-5 M-20 h-S	-	58.2	3.3	36.0	2.5	303	0.111	0.77	4.08	3.31
5-S'	Cel-195-5 M-20 h-S-used	-	58.9	3.3	35.6	2.2	–	–	0.69	n.d.	–
6	Cel-215-2 M-20 h <sup>f</sup>	9.5	74.5	5.1	20.4	–	374	0.168	–	n.d.	–
6-S	Cel-215-2 M-20 h-S	-	52.3	2.5	42.8	2.4	279	0.103	0.73	3.42	2.69
6-S'	Cel-215-2 M-20 h-S-used	-	57.5	3.3	37.1	2.1	–	–	0.67	n.d.	–
7	Cel-195-2 M-40 h <sup>f</sup>	10.0	69.6	4.7	25.7	–	386	0.166	–	n.d.	–
7-S	Cel-195-2 M-40 h-S	-	57.2	3.6	35.4	3.8	283	0.105	1.18	4.27	3.09
8	Cel-195-5M-40h <sup>f</sup>	10.6	75.3	5.6	19.0	–	104	0.045	–	1.28	1.28
8-S	Cel-195-5 M-40 h-S	-	57.7	4.1	34.0	4.2	335	0.125	1.33	2.47	1.14
9	Cel-215-2 M-40 h <sup>f</sup>	17.7	77.2	5.7	17.1	–	170	0.072	–	1.37	1.37
9-S	Cel-215-2 M-40 h-S	-	59.3	4.0	32.4	4.3	347	0.133	1.35	2.90	1.55
9-S'	Cel-215-2 M-40 h-S-used	-	58.0	2.6	37.5	1.9	–	–	0.60	–	–

<sup>a</sup>S<sub>A</sub> = Surface area. <sup>b</sup>V<sub>μP</sub> = Micropore volume. <sup>c</sup> Calculated from sulfur content. <sup>d</sup> T.A. = total acidity. Determined by back titration. <sup>e</sup> Data from reference [30]. <sup>f</sup> Data from reference [32]. <sup>g</sup> determined by the difference between total acidity and the number of sulfonic sites.

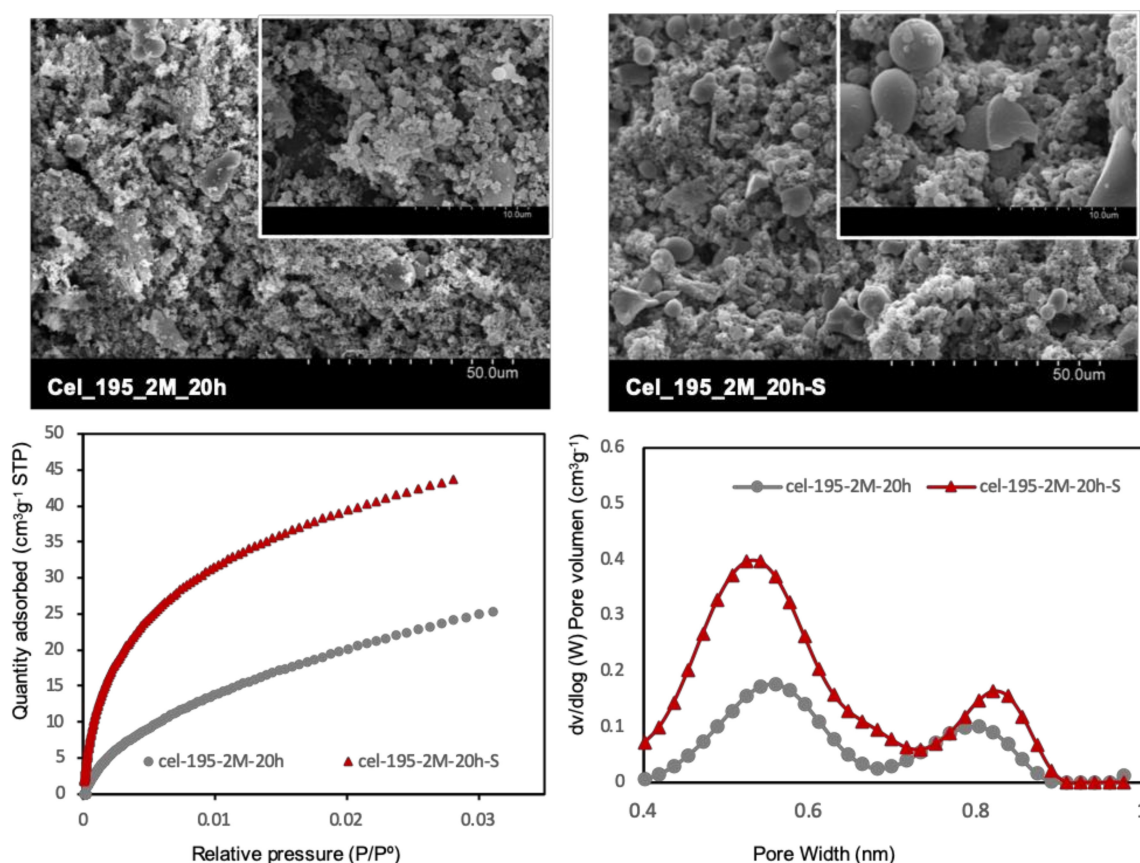


**Figure 1.** Comparison of textural properties of Cel-195-2 M-20 h (sample 3) and Cel-195-2 M-20 h-S (sample 3-S).

CO<sub>2</sub> isotherms adsorption plots and pore width distribution are typical of microporous solids with narrow pores with significant adsorption at low relative pressures [33,34]. The pore size distribution is bimodal with peaks centered at around 0.55 nm and 0.80 nm, that is in the range of ultramicropores. The bimodal shape of the pore size distributions is characteristic for many adsorbents possessing a small amount of micropores and results from the similarity of the local adsorption isotherm in the range of the pore widths for which the gap between peaks (related to the primary and secondary micropore filling mechanism) exists [35].

In spite of the variability of the surface area in the HTC samples, the sulfonation of these solids provided samples with surface areas in a narrower range (224–347 m<sup>2</sup> g<sup>-1</sup>) and with a linear relationship with the hydrothermal index values of the original HTC (Figure 2a), which contrasts with the volcano representation observed for the HTC samples [32]. These facts evidenced that the treatment with sulfuric acid is able to complete the hydrothermal process when this is performed under mild conditions (low H.I.), whereas sulfonation induces a partial degradation of the carbon framework in the case of the carbon samples prepared under harsh conditions (high H.I.), leading to a more open structure with higher surface area and porosity (Table 1). The micropore volume follows a similar linear trend (ESI). As linear trends are observed between H.I. and surface area or micropore volume for SHTC, H.I. based on preparation conditions of original HTC might be of usefulness to predict textural properties of SHTC.

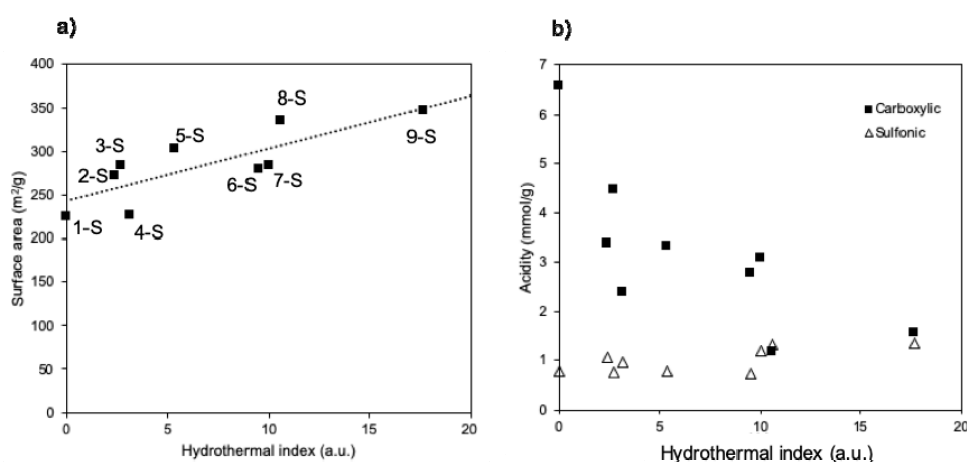


**Figure 2.** Relationship between hydrothermal index (H.I.) from original HTC and properties of SHTC: (a) Surface area; (b) sulfonic and carboxylic acidity (determined by difference between total acidity and a sulfonic acidity).

In terms of solid composition, and as expected, sulfonation increases the oxygen content (Table 1), which is also confirmed by XPS. In the C1s spectrum, the contributions of C–O (286.2 eV), C=O (287.3 eV) and COOH (289.0 eV) bonds [36] increase with respect to that of C without bonds to oxygen (284.6 eV) (Figure 3a), whereas in the O1s spectrum the contribution of C=O (531.6 eV) increases with respect to the other oxygenated groups (Figure 3b), confirming in this way the partial oxidation of HTC upon sulfonation.

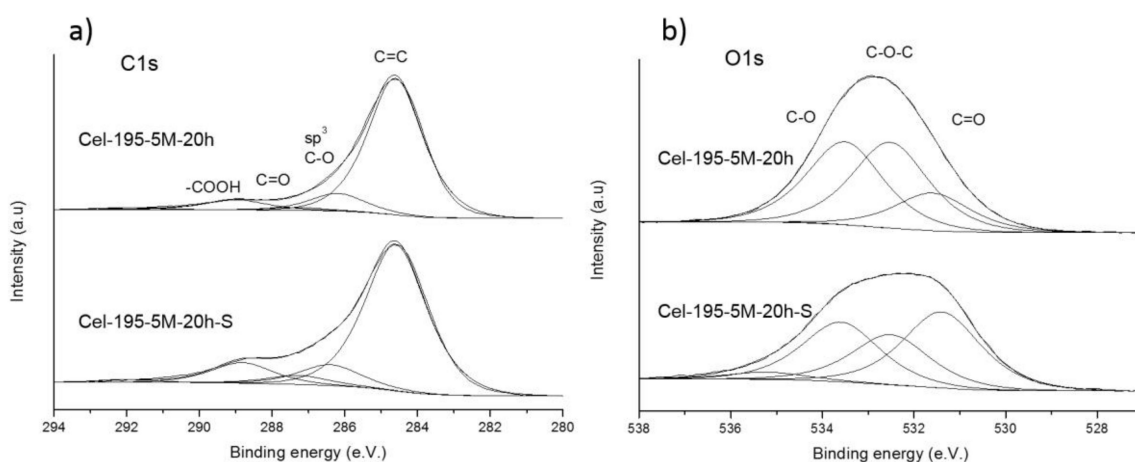


**Figure 3.** XPS spectra of Cel-195-5 M-20 h and Cel-195-5 M-20 h-S (samples 5 and 5-S, respectively): (a) C1s; (b) O1s.

The carbon/oxygen composition of the SHTC based on cellulose is linear with the hydrothermal index (H.I., Figure 4a), and the lines for both carbon and oxygen are nearly parallel to those of the non-sulfonated HTC samples (Figure 4a). Thus, harsher hydrothermal conditions produce higher deoxygenation of the generated HTC, a trend that is reproduced in the corresponding SHTC. However, the effect is not so linear in the case of sulfur content, which shows a larger variability (Figure 4b). The explanation for this behavior is not straightforward, as the sulfonation of the aromatic groups takes place at the same time as other side reactions and strongly depend on the chemical nature of the solids, which present different features as it will be shown in NMR study (Figure 5).

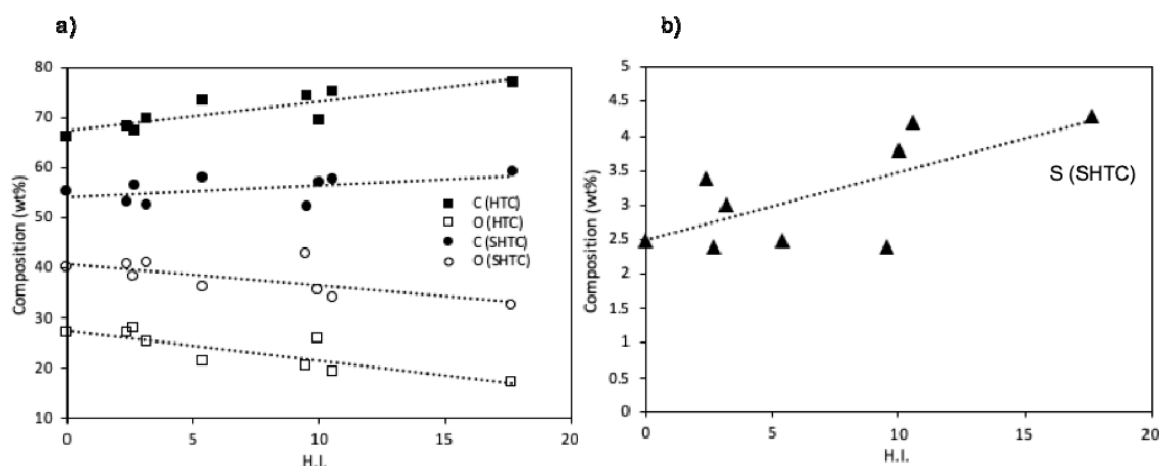


**Figure 4.** Relationship between hydrothermal index (H.I.) of HTC and composition of HTCs and SHTCs: (a) Carbon and oxygen content (wt%); (b) sulfur content (wt%).

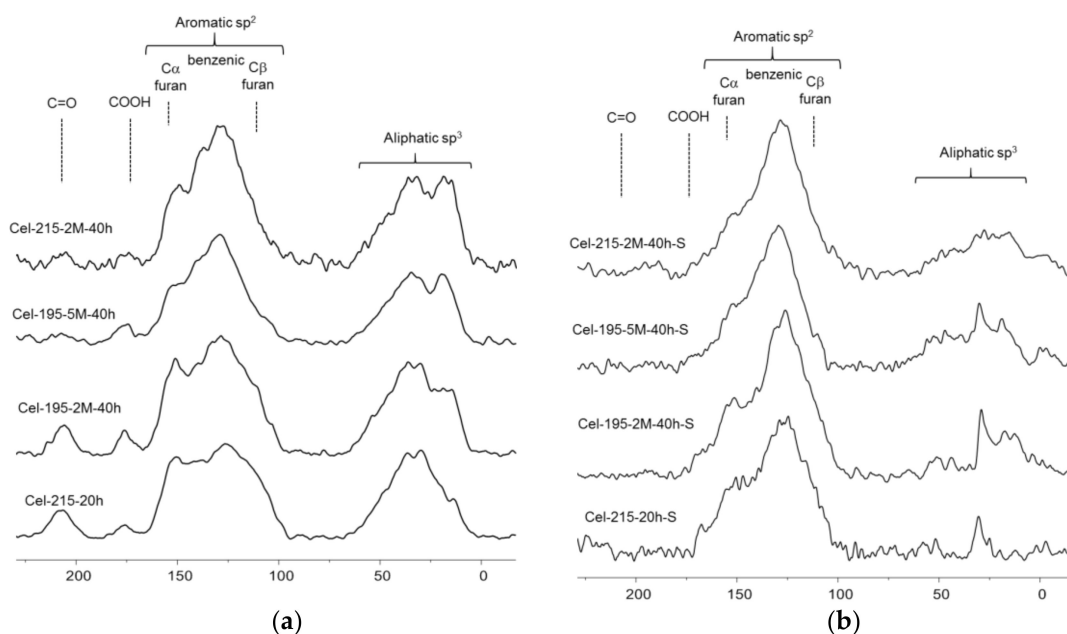


**Figure 5.** <sup>13</sup>C-CP-MAS-RMN spectra of: (a) HTC (samples 4, 7, 8, 9); (b) SHTC (samples 4-S, 7-S, 8-S, 9-S).

This sulfur content (Table 1 and Figure 4b) indicates sulfonic acidities in the range of 0.75–1.35 mmol/g, with a certain dispersion but slight increasing trend with H.I., which contrasts with the case of carboxylic acidity (Figure 2b), calculated by the difference between total acidity (determined by titration) and number of sulfonic groups (calculated from sulfur analysis). The materials prepared under harsher conditions (higher hydrothermal index) present significantly lower acidity, in agreement with the lower oxygen content (Figure 4a), which would indicate the formation of higher aromatic and condensed materials.

As previously described [32], <sup>13</sup>C-CP-MAS-NMR spectra of HTC from cellulose show three main types of carbon atoms: carbonyl groups (C=O and COOH), aromatic sp<sup>2</sup> carbons and aliphatic sp<sup>3</sup> carbons (Figure 5a). Upon sulfonation, the spectra of SHTC samples (Figure 5b) show in all the cases a drastic reduction in the contribution of aliphatic groups, together with a decrease in the contribution of carbonyl groups, and a higher graphitization degree, shown by the lower contribution of furanic aromatic carbons. These results seem to be contradictory with the increase in oxygen content determined by elemental analysis and XPS. However, the spectra of HTC and SHTC are not directly

comparable, as they were registered using the cross-polarization (CP) technique, which enhances the signal of the carbon atoms close to hydrogen atoms. The sulfonation also produces a decrease in the hydrogen content of the hydrothermal carbons, a consequence of the larger condensation and graphitization processes, lowering in this way the intensity of the  $^{13}\text{C}$ -CP signals.

The analysis of the nature of the acid sites on the solids has been carried out by  $^{31}\text{P}$ -MAS-NMR using triethyl phosphine oxide (TEPO) as probe molecule (Figure 6). The spectra show a very broad signal in the range of 50–95 ppm due to the contribution of different acidic sites. The signal deconvolution evidences the presence of arylsulfonic sites at 82–85 ppm [37,38], although in a much lower contribution than expected. In fact, the contribution of carboxylic sites (signal at 60–64 ppm [37]) is also important. However, a signal at 70–73 ppm, in the range of alkylsulfonic sites [37,38], appears as the major contribution in some of the spectra (Figure 6). In fact, this signal had been already detected by other authors, but it has not been interpreted [39], as it is difficult to envisage the formation of such kind of sites in a sulfonation process with sulfuric acid, that should take place on aromatic groups (electrophilic aromatic substitution) leading to arylsulfonic sites. Given that the adsorbed TEPO/ $\text{SO}_3\text{H}$  molar ratio is only 0.8, and taking into account the big difference in  $\text{pK}_a$  between sulfonic and carboxylic acids, the important signal at 60–64 ppm seems to indicate the existence of diffusion limitations to get access to part of the sulfonic sites, at least in the adsorption conditions (r.t., methanol as solvent), that may condition the catalytic activity of the SHTCs. This fact is due to the flexibility of these materials, which strongly depends on the polarity of the media, as it has been previously shown for Glu-195-20 h [31].

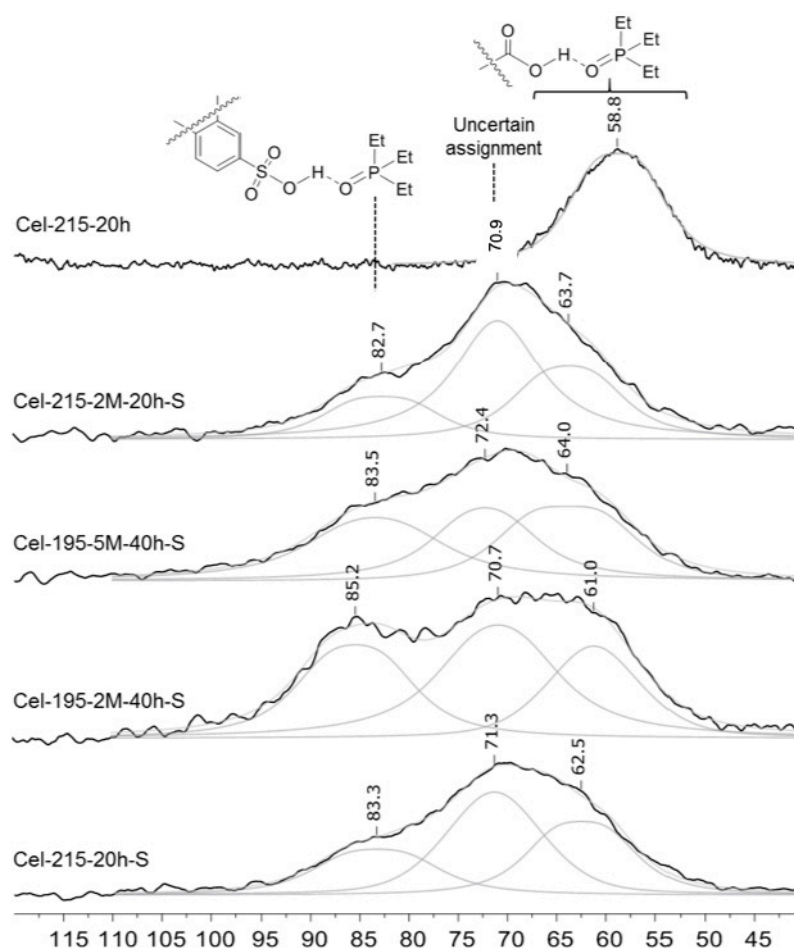


**Figure 6.**  $^{31}\text{P}$ -MAS-NMR spectra of TEPO adsorbed on one HTC sample (Cel-215-20 h, sample 4) and SHTC (samples 6-S, 8-S, 7-S, and 4-S from the top to the bottom).

## 2.2. SHTC on Graphite Felt: Preparation and Characterization

In a previous work [12], we described the preparation of SHTC-covered graphite felt (SHTC@GF) from glucose and its characterization by different methods. SEM images showed that the felt microfibers were homogeneously coated by a 300–350 nm HTC layer, which was stable to sulfonation. The SHTC loading was determined from the weight loss in TPO-MS (Temperature Programme Oxidation- Mass Spectroscopy) experiments

Although the SHTC@GF samples could also be used in batch reactors, the main purpose for these samples in this work to demonstrate the reactions in continuous flow reactors. Thus, the felt mats of 5 mm thickness were cut into disks of 16 mm of diameter (Figure 7) to allow the tightly fitting inside the reactor (Figure 7). In this way, the length of the bed can be increased by numbering up several felt disks in a pile. To convert the graphite felts into the structured catalyst SHTC@GF, the microfibers were coated by a HTC layer and then sulfonated as described in the experimental section.

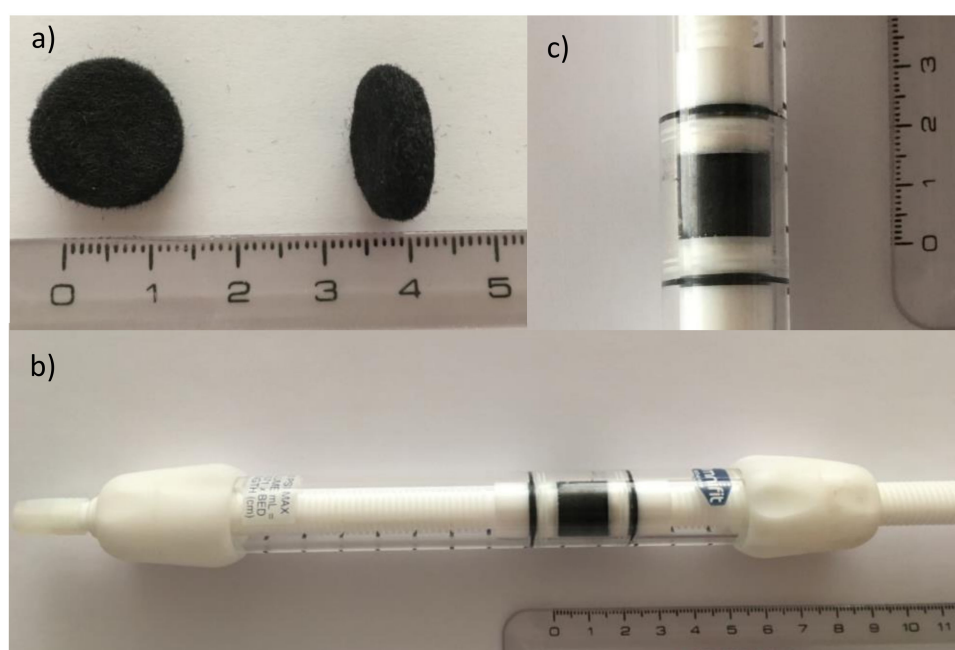


**Figure 7.** Disks of SHTC@GF (a) reactor with three tightly piled disks (b) and enlarged image of the piled disks (c).

The percentage of hydrothermal carbon coating was estimated by TPO-MS. The weight loss in the range of 300–500 °C was 19.4 wt% which corresponds to HTC, whereas the graphite felt starts to burn out above 610 °C. The sulfur content of SHTC@GF was 0.3 wt%, corresponding to a sulfur loading on the SHTC coating of 0.48 mmol g<sup>-1</sup>, lower than the content in unsupported SHTC, 0.77 mmol g<sup>-1</sup> (Table 1 sample 1-S). This suggests that the sulfonation process is more effective in the powdered sample than in the HTC@GF.

The graphite felt was also covered with Cel-215-2 M-20 h (sample 6), the SHTC from cellulose that led to the best catalytic results in batch reactions (see Section 2.3). In this case, the carbon coating was estimated to be 21.0% by TPO-MS. The sulfur content was 0.29 wt%, corresponding to a sulfur loading on the SHTC coating of 0.43 mmol g<sup>-1</sup> similar to the functionalization of SHTC@GF and again lower than the one of the powdered sample, 0.73 mmol g<sup>-1</sup> (Table 1, sample 6-S), thus confirming a more difficult sulfonation of hydrothermal carbons coated on felts.

## 2.3. Catalytic Performance of SHTCs in the Synthesis of Solketal: Batch Reactions

The SHTCs were tested as catalysts in the synthesis of solketal (Scheme 1) at 25 °C using an acetone: glycerol molar ratio of 7:1 and 1 wt% of the catalyst with respect to glycerol. Solketal yields

were determined by GC. As functionalization of the SHTCs was different, the initial glycerol/SO<sub>3</sub>H ratio varied from 823 to 1522. Thus, their catalytic activity is compared using initial TOF (Turn Over Frequency) values (h<sup>-1</sup>) (evolution of solketal yields with time is gathered in supplementary information). A broad dispersion of the results was obtained, from 193 h<sup>-1</sup> for Cel-195-2 M-40 h-S (sample 7-S in Table 1, H.I. 10.0) up to 2194 h<sup>-1</sup> for Cel-215-2 M-20 h-S ((sample 6-S in Table 1, H.I. 9.5) and with an activity result (571 h<sup>-1</sup>) for Glu-195-20 h-S ((sample. 1-S, H.I. 0.0). From the results obtained it is difficult to find a clear relationship between the catalytic activity and any of the parameters obtained by the different characterization techniques (acid content, surface area, pore volume, acid density, acidity both total and sulfonic, and hydrothermal index). The plot of TOF vs. sulfonic content is represented in Figure 8. It seems that there is a trend of decrease in activity for increasing sulfonic content, with the catalysts prepared from cellulose with HCl for 20 h as the most active ones. Interestingly, the other two catalysts with better performance than Glu-195-20 h-S are also those prepared from cellulose for 20 h of hydrothermal synthesis. As pointed by the <sup>31</sup>P-NMR experiments of TEPO adsorption, part of the sulfonic sites seems not to be accessible for this probe molecule, depending on the nature of the SHTC. The situation is even more complicated in the case of the reaction, as acetone and glycerol are only partially miscible and the adsorption of both reactants might be conditioned also by the hydrophilicity/hydrophobicity character of the catalyst. This fact would introduce an unknown factor to the catalytic activity, and probably the hydrothermal synthesis for longer times is detrimental in this respect.

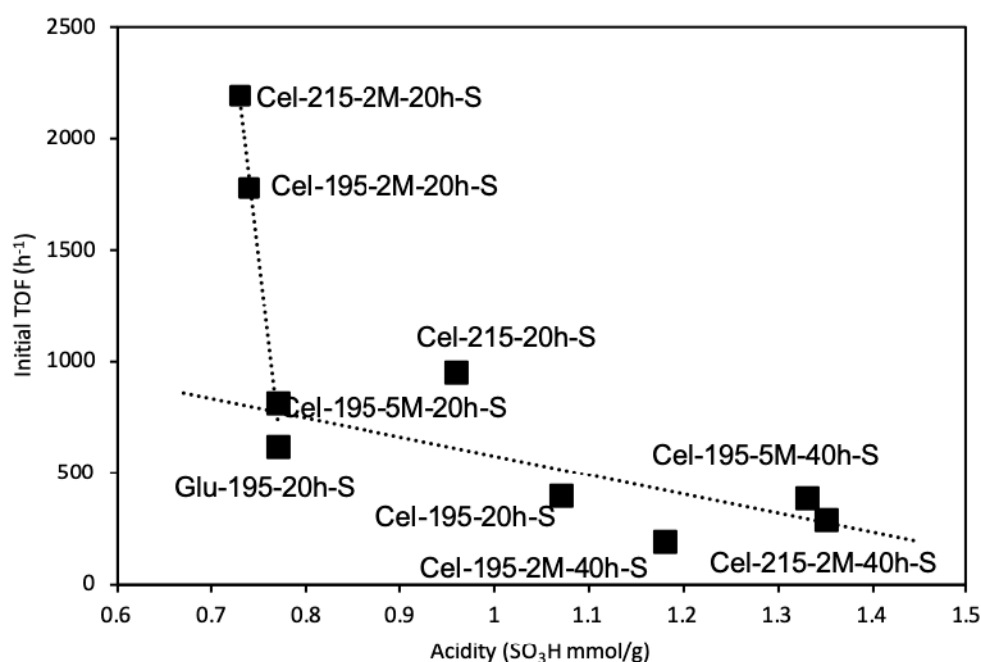


**Figure 8.** Initial TOF in solketal synthesis vs. sulfonic acidity plot with fresh SHTCs as catalysts (reaction conditions: acetone: glycerol molar ratio 7:1, catalyst 1% *w/w* with respect to glycerol, 25 °C).

In all the cases, yields in the range of 80–86% were obtained after 2–4 h, depending on the nature of the SHTC. It is noteworthy that these yields are comparable to previously described in the literature with different heterogeneous catalysts [25,29], but in our case reactions were carried out at r.t. while reactions with activated carbons and zeolites are described at 80 °C and 70 °C, respectively.

In order to compare the activity of SHTC with commercial sulfonic solids, two arylsulfonic resins (Dowex 50Wx2 and Amberlyst A15), Nafion-silica SAC-13 with perfluoroalkylsulfonic sites, and Deloxan ASP with alkylsulfonic sites were tested in the solketal synthesis using the same reaction conditions as with SHTCs (see experimental section). These commercial catalysts showed similar or significantly lower activity per sulfonic site, an effect that had been already observed in esterification

reactions [37,40]. The activity of aryl sulfonic resins seems to depend on the cross-linking degree, with values similar to those of the SHTCs for the resin with low cross-linking degree ( $653\text{ h}^{-1}$  for Dowex 50W with 2% cross-linking) and very poor catalytic activity with a macroreticular resin ( $35\text{ h}^{-1}$  with Amberlyst 15). This effect evidences the importance of the swelling of the resin in order to facilitate the accessibility to the catalytic sites, thus Dowex 50Wx2 with a lower crosslinking degree has a bigger swelling capability that allowed a better diffusion of the reactants and a better accessibility to the active sites. Perfluoroalkyl sulfonic sites do not show better activity in spite of their stronger acidity and the lack of diffusion problems in Nafion-silica SAC-13 ( $408\text{ h}^{-1}$ ). Alkyl sulfonic sites also display lower activity ( $148\text{ h}^{-1}$  with Deloxan ASP) in agreement with their weaker acidity. Weaker acid sites, such as carboxylic acids present in an acrylic resin (Dowex CCR2), were not active at all. (plots of productivity values, calculated as mmol of solketal produced per mmol of sulfonic sites, vs. time for these reactions are gathered in the ESI).

A deactivation mechanism of Glu-195-20 h-S based on the esterification of the surface acid sites, promoted by their close proximity, was evidenced by  $^{13}\text{C}$ -CP-MAS-NMR when this catalyst was used in the esterification of fatty acids in methanol at high temperature [30,33]. However, the mild conditions of temperature in the solketal synthesis ( $25\text{ }^{\circ}\text{C}$ ) seemed to be favorable for an efficient recovery and reuse of the SHTCs. Surprisingly, Glu-195-20 h-S was strongly deactivated as the initial TOF decreased from 618 to 0 in the second run (Figures 8 and 9). On the contrary, the SHTCs from cellulose were recoverable. TOF values for reused catalysts (calculated with the functionalization data from the non-used catalyst) are shown in Figure 9. As it can be seen, a narrower range of TOF values was observed than in the case of the first run (fresh catalysts), with values between  $548$  and  $800\text{ h}^{-1}$ , and only one exception, Cel-195-5 M-20 h-S (sample. 5-S in Table 1, H.I. 5.4) with TOF of  $1048\text{ h}^{-1}$ . Similar values of TOF are obtained when using the functionalization values of the used catalysts for its calculation (see Figure S18 in ESI). This seems to indicate that, in spite of the very large amount of water used for washing during the preparation of SHTC, the best fresh catalysts may still retain some weakly adsorbed sulfuric acid, which is removed during their first use in the solketal synthesis. This is evidenced by the loss of sulfur observed in used SHTCs samples (Table 1). On the contrary, the improvement upon recycling of the worst fresh catalysts might be explained by some kind of pore clogging produced during preparation, which might be removed in the first reaction, and hence all the catalysts show a similar performance in the second run. Plots of productivity values (mol of solketal produced per mol of sulfonic sites) vs. time upon reuse for all the catalysts are provided in the supplementary information. From the results herein described, no relationship between TOF of the reused catalysts and the loss of sulfur could be established, indicating that the loss of active sites by leaching was not the only deactivation mechanism. Other possible reasons for the changes in TOF values for fresh and reused catalysts might be the adsorption of glycerol on the highly hydrophilic catalyst, the chemical reaction of the acidic sites [30,37] or the pore blocking due to by-products adsorption; however, due to the low temperature reaction conditions (r.t), the most probable deactivation mechanism is more likely to be the adsorption of glycerol or by-products on the surface of the catalyst.

Finally, it is noteworthy that the SHTC, from cellulose, performed reasonably well even at room temperature in the synthesis of solketal, and the TOFs herein described (from  $193$  to  $2194\text{ h}^{-1}$ ) are relatively high and comparable to the ones of commercial sulfonic resin Dowex 50Wx2 described in this work ( $653\text{ h}^{-1}$ ).

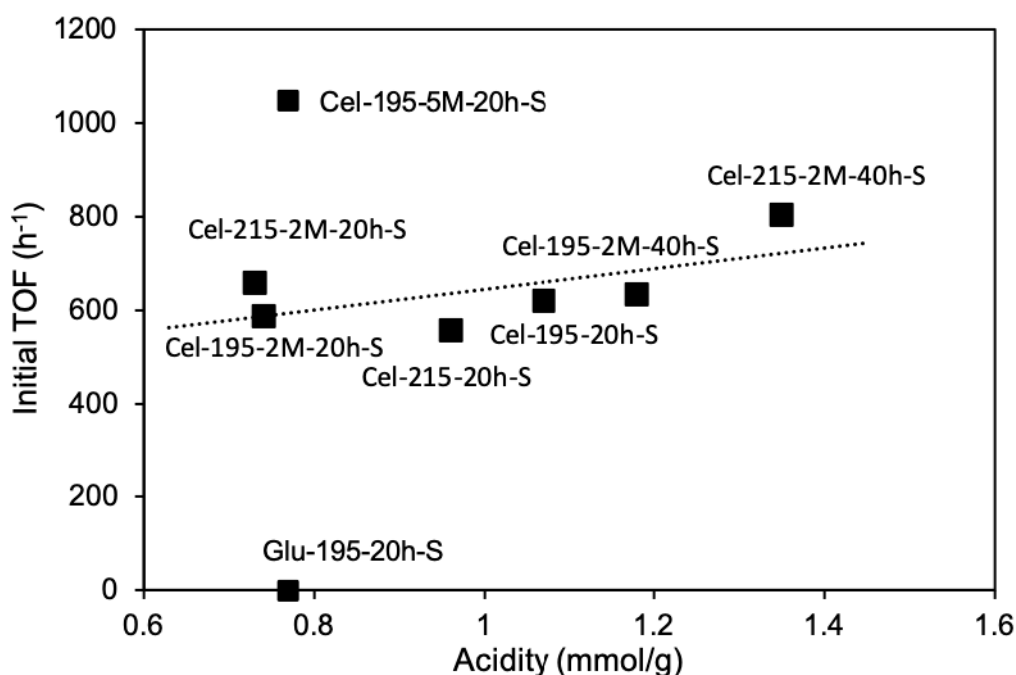


**Figure 9.** Initial TOF in solketal synthesis vs. sulfonic acidity plot with second-used SHTC as catalyst (reaction conditions: acetone: glycerol molar ratio 7:1, catalyst 1% *w/w* with respect to glycerol, 25 °C).

#### 2.4. Catalytic Performance of SHTC in the Synthesis of Solketal: Continuous Flow Reactions

Once all the SHTC solids were tested and proved their activity in the reaction of glycerol with acetone, two of the catalysts were selected in order to carry out continuous flow reactions for the synthesis of solketal: the best SHTC coming from cellulose, Cel-215-2 M-20 h-S (sample 6-S in Table 1, H.I. 9.5) and Glu-195-20 h-S (sample 1-S in Table 1), in order to compare two carbons from different sources. Thus, graphite felts covered with Glu-195-20 h-S and Cel-215-2 M-20 h-S were tested in the continuous acetalization of glycerol and acetone at 25 °C using the reactor shown in Figure 7 and the flow system described in the Materials and Methods section.

In the developing of a continuous production of solketal, parameters such as acetone/glycerol molar ratio and flow rate were optimized using the Glu-195-20 h-S@Graphite Felt. As described in the experimental section, SHTC@GF disks were stacked inside the reactor, through which glycerol and acetone passed and reacted. We carried out two sets of experiments at 25 °C with two different acetone/glycerol molar ratios, 9:1 and 4:1, while varying the weight hourly space velocity (WHSV) of glycerol in between 336 and 1680 g glycerol h<sup>-1</sup> g<sup>-1</sup> of catalyst (Figure 10).

The results show that glycerol conversion declined as the WHSV increased, but passing through a maximum at an intermediate value which depended on the acetone/glycerol molar ratio. For example, the solketal productivity (mmol of solketal produced per gram of hydrothermal carbon per hour) exhibited a maximum of 2048 mmol g<sup>-1</sup> h<sup>-1</sup> for an intermediate WHSV of 1175 g of glycerol h<sup>-1</sup> g<sup>-1</sup> of catalyst with an acetone/glycerol ratio of 9, whereas for an acetone/glycerol molar ratio of 4 the maximum productivity was 671 mmol g<sup>-1</sup> h<sup>-1</sup> for an intermediate WHSV of 627 g of glycerol h<sup>-1</sup> g<sup>-1</sup> of catalyst. Considering these results, a ratio of acetone/glycerol 9:1 and a WHSV of 1175 h<sup>-1</sup> were selected to carry out a preliminary study of solketal productivity vs. time.

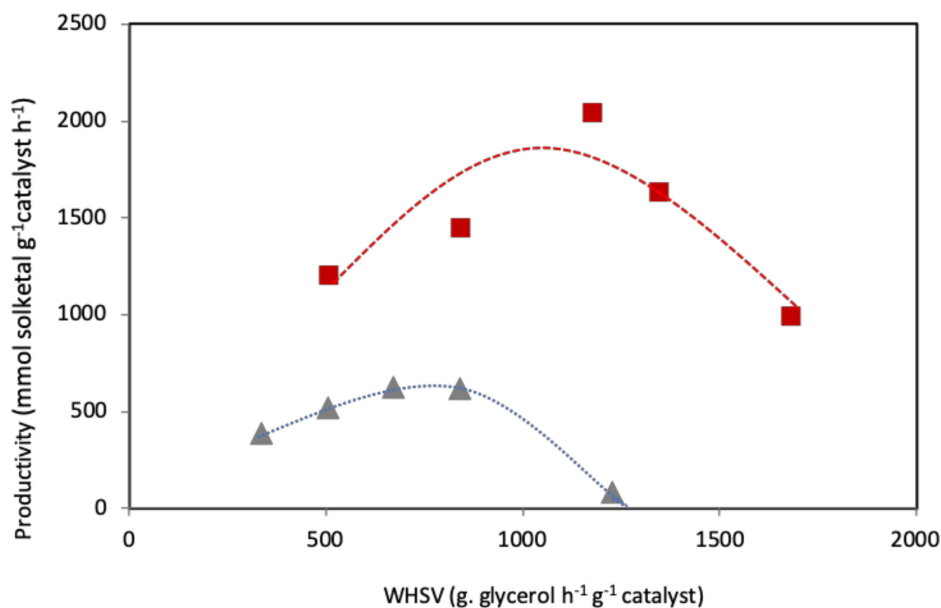


**Figure 10.** Solketal productivity as a function of WHSV for constant acetone/glycerol ratios of 9:1 (■) and 4:1 (▲). (Reaction conditions: 45 mg of Glu-195-20 h-S deposited on GF, 25 °C, residence time 1 min).

Figure 11 shows that solketal productivity (defined as moles of product per g of catalyst and per hour) for the Glu-195-20 h-S based catalyst decreased gradually with time on stream, with almost complete deactivation after only 1 h. The temperature programmed oxidation of the used catalyst (Glu-195-20 h-S@GF) showed a 65% weight loss at 170–200 °C, which can be unambiguously ascribed to the accumulation of glycerol on the structured catalyst since the flash point of glycerol is 176 °C. Therefore, the accumulation of unconverted glycerol on the catalyst surface, appears to be due to the high hydrophilicity of the SHTC and the high viscosity of glycerol, resulting in the blocking of the catalytic sites and deactivation of the catalyst under flow conditions, which can also explain the deactivation of the catalysts in the case of batch reactions. In fact, when the deactivated catalyst (Glu-195-20 h-S@GF) was washed with hot water at 60 °C for 30 min at a flow of 3 mL/min, in order to remove glycerol in the solid, the activity was partially recovered, thus confirming the hypothesis of the presence of glycerol blocking the catalytic sites and the need of a regeneration step under these reaction conditions.

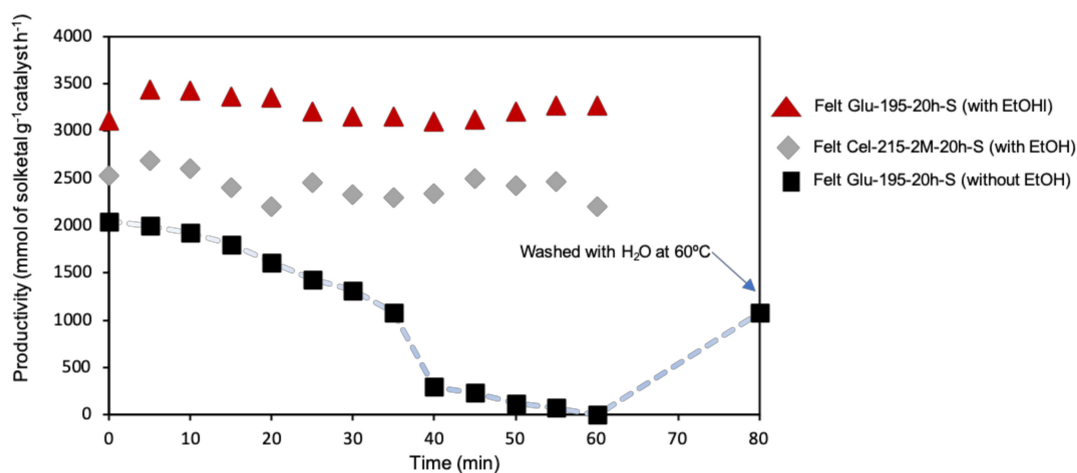


**Figure 11.** Solketal productivity in continuous flow at 25 °C using 10 mmol/min of glycerol (WHSV 1175 h<sup>-1</sup>) and acetone/glycerol molar ratio of 9.

In order to overcome deactivation by glycerol adsorption and the need of catalyst regeneration, EtOH (20% *v/v*) was fed together with the mixture of acetone and glycerol. In this way, reactants dilution and mixing in one single liquid phase is favored (since acetone and glycerol are only partially miscible) which resulted in a relatively constant solketal productivity in between 3100 and 3500 mmol g<sup>-1</sup> of catalyst h<sup>-1</sup> maintained for 1 h (Figure 11), indicating that this strategy also prevented the accumulation of unconverted glycerol on the catalyst, at least at short times on stream. This productivity is much higher than the initial one using SHTC@GF in a batch process in the same conditions (ca. 1770 mmol g<sup>-1</sup> of catalyst h<sup>-1</sup> in 15 min residence time). These productivities are far higher than previous ones described in the literature [23], where a productivity of 20.65 (mmol of solketal g<sup>-1</sup> of catalyst h<sup>-1</sup>) was achieved using Amberlyst 36 as catalyst with a WHSV of 2 g of glycerol g<sup>-1</sup> of catalyst h<sup>-1</sup>, a molar ratio of acetone/glycerol 4:1 and at 25 °C.

Finally, felts covered with Cel-215-2 M-20 h-S were also tested in the flow reaction using optimized conditions. In this case, productivities similar to those obtained with Glu-195-20 h-S@GF were achieved, resulting in steady performance for 1 h time on stream (Figure 11). Contrary to what has been observed in batch reactor, higher productivities were obtained when using Glu-195-20 h-S@GF. In this case, deposition of the carbon over the felt can slightly modify textural properties and accessibility to sulfonic sites, thus modifying the activity of the catalyst to some extent.

Overall, these results demonstrate the utility of using this type of supported sulfonated hydrothermal carbons in order to implement continuous flow systems for the production of biomass derived chemicals, such as solketal.

### 3. Materials and Methods

Sulfuric acid (>95%, Fischer, Madrid, España), acetone (99.8%, Fischer), absolute ethanol (Labkem-Labbox, Villasar de Dalt, Barcelona, España), glycerol (99.5%, Sigma-Aldrich, Madrid, España), microcrystalline cellulose (Merck, Kenilworth, NJ, USA) and 1-methyl-naphtalene (96%, Alfa Aesar, Ward Hill, MA, USA) were used as received without further purification. The catalysts Dowex 50Wx2, Amberlyst 15, Nafion-silica SAC-13 and Dowex CCR2 were purchased from Sigma-Aldrich, and Deloxan ASP was purchased from Degussa (Frankfurt, Germany).

#### 3.1. Catalysts Synthesis and Characterization

Glucose sulfonated hydrothermal carbon was prepared in a two-step procedure: hydrothermal synthesis at 195 °C and sulfonation with concentrated sulfuric acid at 150 °C [30]. The carbon preparation from cellulose follows a similar procedure, in this case HCl can be used to favor the pre-hydrolysis of the raw material [32]. For simplicity, all the solids are noted in the main text indicating their origin (glucose by Glu, or cellulose by Cel) and the preparation conditions such as temperature (195 °C or 215 °C), concentration of HCl acid (2 M or 5 M) and time of hydrothermal treatment (20 h or 40 h).

In a typical procedure, 2 g of microcrystalline cellulose in 10 mL of pure distilled water (alternatively, 10 mL of either 2 M or 5 M HCl solution were used) were introduced in a 40 mL Teflon-lined autoclave. The autoclave was closed and introduced in an oven at the desired temperature (195 °C or 215 °C) and it was maintained inside the oven during the desired time (20 h or 40 h). The obtained carbon was filtered off and thoroughly washed with water and acetone. Subsequently, the carbons were treated with concentrated (>96%) sulfuric acid (20 mL H<sub>2</sub>SO<sub>4</sub>/g solid) in a round-bottom flask furnished with a reflux condenser under argon atmosphere for 15 h at 150 °C. The sulfonated samples were then washed thoroughly with hot distilled water and acetone and dried in an oven overnight in static air at 105 °C.

A 5 mm-thick graphite felt (GF) sheet was cut into 16 mm diameter circular pieces, which were washed with acetone and treated with nitric acid (65%) in a flask furnished with a reflux condenser with gentle stirring at 80 °C for 16 h. The hydrothermal carbon covered graphite felt (HTC@GF) was prepared from GF and glucose or cellulose by hydrothermal synthesis into an autoclave vessel, followed by sonication in water for 10 min and final washing with ethanol to eliminate the hydrothermal carbon

loosely bound to the graphite felt. The sulfonation step was carried out under the same conditions used for the HTC, which led to the formation of SHTC@GF. Additional experimental details have been described elsewhere [12].

The obtained solids were characterized by the following techniques. Elemental analysis (C,H,S), were carried out in an Thermofisher Flash 1112 elemental analyzer (Waltham, MA, USA) and CO<sub>2</sub> adsorption was carried out for surface area and pore volume distribution determination. CO<sub>2</sub> adsorption (Dubinin-Radushkevich) was determined at 0 °C using a Micromeritics ASAP 2020 apparatus (Norcross, GA, USA) after outgassing for 4 h at 150 °C. For the estimation of the surface area, the Dubinin–Astakhov equation was used.

Scanning electron microscopy (SEM) was carried out with a SEM EDX Hitachi S-3400 N microscope (Tokyo, Japan) with variable pressure up to 270 Pa and with an EDX Röntec XFlash of Si(Li) analyzer (Berlin, Germany). The samples were sputtered with gold previously to measurements and the images were obtained from the secondary electron signal. The mean particle size was determined by measuring 100 particles from images at different locations of the sample.

XPS spectra were recorded with an ESCAPlus Omnicrom system (Taunusstein, Germany) equipped with an Al K radiation source to excite the sample. Calibration of the instrument was done with Ag 3d5/2 line at 368.27 eV. All measurements were performed under UHV, better than 10–10 Torr. Internal referencing of spectrometer energies was made using the dominating C 1s peak of the support at 284.6 eV. The program used to do curve fitting of the spectra was CasaXPS using baseline Shirley method.

Back titration with NaOH was used for the determination of the total amount of acid sites. The solid sample (30 mg) was added to 25 mL of 0.01 M NaOH solution and allowed to equilibrate under stirring for 1 h. Thereafter, it was titrated with 0.05 M potassium hydrogen phthalate solution using a Crison pH Burette 24. The use of potassium hydrogen phthalate (pKa 5.4) avoids the reaction of this acid with the neutralized acid sites on the solid, thus precluding the underestimation of the acid sites, besides it avoids the filtering of the solid before titration that might be sources of errors in the site determination.

Total acid density was defined as the number of total acid sites per m<sup>2</sup> and calculated from titration values and surface area data.

Sulfonic sites density was defined as number of sulfonic sites per m<sup>2</sup> and calculated from sulfur content and surface area data.

Solids were also studied by <sup>13</sup>C-CP-MAS-NMR (cross polarization–magic angle spinning–nuclear magnetic resonance). NMR spectra were recorded in a Bruker Avance III WB400 spectrometer (Billerica, MA, USA) with 4 mm zirconia rotors spun at magic angle in N<sub>2</sub> at 10 kHz. <sup>1</sup>He-<sup>13</sup>C CP (cross-polarization) spectra (up to 10,000 scans) were measured using a <sup>1</sup>H π/2 pulse length of 2.45 μs, with a contact time of 2 μs, and spinal-64 proton decoupling sequence with a pulse length of 4.6 μs.

Triethylphosphine oxide (TEPO) adsorption and <sup>31</sup>P-MAS-NMR analysis were also carried out. In a typical procedure, 25 mg of SHTC was suspended in a TEPO methanol solution. The mixture was stirred for 2 h, the solvent was removed by vacuum distillation and the solid TEPO-SHTC sample was analyzed by NMR.

### 3.2. Acetalization Reactions of Glycerol with Acetone Catalyzed by SHTC in a Batch Reactor

In a typical catalytic test, 4.5 g (0.05 mol) of highly purified glycerol, 25 mL of acetone (0.34 mol, 1 wt% (45 mg) of the catalyst and 0.675 g of 1-methylnaphtalene (GC internal standard), were weighed in a 50 mL glass round bottom flask. The mixture was stirred at 800 rpm at room temperature. The reaction was monitored by gas chromatography by taking samples were taken at different times, which were diluted in methanol and micro-filtrated prior to injection and analyzed in a Agilent 7890 GC with a FID detector and a Zebron inferno column.

In all cases, the liquid reaction mixture was originally biphasic and became monophasic during the reaction.

After the reaction, the catalysts were filtered off, washed with methanol and acetone and dried at 105 °C overnight before reuse.

In the case of the comparison study of the activity of SHTC with commercial sulfonic solids the amount of catalysts was adjusted depending on the functionalization of the resins Dowex 50Wx2 (4.7 mmol SO<sub>3</sub>H g<sup>-1</sup>), Amberlyst A15 (4.76 mmol SO<sub>3</sub>H g<sup>-1</sup>), Nafion-silica SAC-13 (0.16 mmol SO<sub>3</sub>H g<sup>-1</sup>) and Deloxan ASP (0.8 mmol SO<sub>3</sub>H g<sup>-1</sup>). Thus in a typical experiment, 0.15 mol of highly purified glycerol, 2 g of 1-methylnaphthalene (GC internal standard), 77 ml of acetone and the amount of catalyst corresponding to a 15% mol ratio of sulfonic sites/mol of glycerol were weighed in a 100 mL glass round bottom flask. The mixture was stirred at 800 rpm at room temperature. The reaction was monitored by gas chromatography by taking samples were taken at different times, which were diluted in methanol and micro-filtrated prior to injection and analyzed in an Agilent 7890 GC with a FID detector and a Zebtron inferno column.

In all the cases, TOF was calculated as mol of glycerol reacted per hour and per mol of sulfonic sites, as carboxylic sites were not active in this reaction as it is demonstrated by the lack of activity of carboxylic resin Dowex CCR2 and non-sulfonated HTC (Glu-195-20 h), whereas productivity was calculated as mol of solketal per mol of sulfonic sites.

### 3.3. Acetalization Reaction of Glycerol with Acetone in a Continuous Flow Reactor

The continuous acetalization of glycerol with acetone was carried out in a flow system, as that schematized in Figure 12. The reactor was an Omnifit® chromatography column 15 mm in internal diameter and a variable length of up to 100 mm where three SHTC felts were stacked (ca. 75 mg of SHTC). The tubing was 1.6 mm O.D. made of PTFE and connected with luer type connections. The reaction was performed at room temperature and atmospheric pressure. Glycerol and acetone were fed with a “Gemini 88” infusion pump through two independently controlled glass syringes with a total flow from 2 to 17 ml/min. For the case of a single homogeneous liquid phase, glycerol and acetone were previously mixed and 20% v/v of absolute EtOH was added. A total flow of 5 ml/min was used. The reaction samples were collected each minute in sealed vials, diluted in methanol and analyzed by GC using 1-methylnaphthalene as standard.

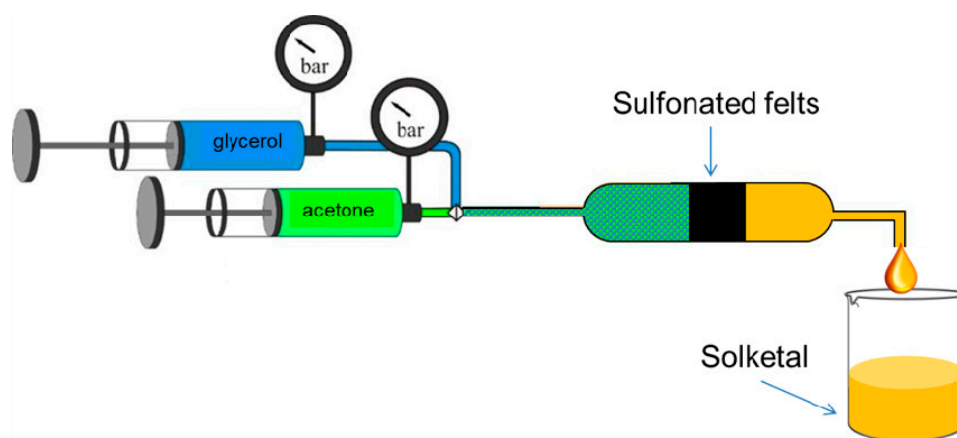


**Figure 12.** Experimental set-up for continuous production of solketal in a flow reactor.

The reaction products were analyzed by gas chromatography (GC) using an Agilent 7890 GC with a FID detector and a Zebtron inferno column.

## 4. Conclusions

Active carbon-based acid catalysts were prepared by hydrothermal treatment of glucose and cellulose and their subsequent sulfonation. It was found that the starting material (glucose or cellulose) and the synthesis parameters strongly influenced the nature of the carbon catalyst. All the sulfonated

carbons showed a high activity in the synthesis of solketal at room temperature in a batch reactor, this activity was comparable to the one by Dowex 50Wx2 resin and higher than the ones obtained with Amberlyst 15, Deloxan or composites such as Nafion-silica-SAC-13. Differences in initial TOFs observed for the sulfonated carbons were difficult to relate to any structural parameter (acid content, surface area, pore volume, acid density, acidity both total and sulfonic, and hydrothermal index). Nevertheless, the solids obtained at longer hydrothermal treatment times were generally less active, probably due to a poor access of the reactants to catalytic sites. The use of felts covered with sulfonated carbons derived from both glucose and cellulose allowed the design of a flow system for continuous solketal production. The use of ethanol in the feeding mixture was crucial to avoid catalyst deactivation and to maintain solketal productivity at least at short times on stream (one hour).

**Supplementary Materials:** The following are available online at <http://www.mdpi.com/2073-4344/9/10/804/s1>, Hydrothermal index definition, SEM images of HTC and SHTC, Plots of CO<sub>2</sub> adsorption isotherms and pore distribution of HTC and SHTC, Relationship between H.I. and micropore volume, Productivity vs time plots for the synthesis of Solketal catalyzed by sulfonated hydrothermal carbons from cellulose prepared at 195 °C, Productivity vs time plots for the synthesis of Solketal catalyzed by sulfonated hydrothermal carbons from cellulose prepared at 215 °C, Productivity vs time plots for the synthesis of Solketal catalyzed by commercial resins and Glu-195-20 h-S, Initial TOF in solketal synthesis vs sulfonic acidity of reused catalyst plot with second-used SHTC as catalyst.

**Author Contributions:** E.G.-B. was responsible for hydrothermal carbon synthesis, J.M.F. carried out catalyst characterizations and E.P. and P.F. performed catalytic tests. J.M.F., E.G.-B. and E.P. are responsible for conceptualization and discussion of the results and contributed equally to the writing and design of the manuscript. J.M.F. and E.G.-B. secured funding for the research work.

**Funding:** Financial support from Ministerio de Ciencia, Innovación y Universidades (project RTI2018-093431-B-I00 and ENE2016-79282-C5-1-R) and the Gobierno de Aragón (Group E37\_17R) co-funded by FEDER 2014-2020 “Construyendo Europa desde Aragón” is acknowledged.

**Conflicts of Interest:** The authors declare no conflict of interest.

## References

1. Abate, S.; Lanzafame, P.; Perathoner, S.; Centi, G. New Sustainable model of biorefineries: Biofactories and challenges of integrating bio- and solar refineries. *ChemSusChem* **2015**, *8*, 2854–2866. [[CrossRef](#)] [[PubMed](#)]
2. Bobleter, O.; Niesner, R.; Röhr, M. The hydrothermal degradation of cellulosic matter to sugars and their fermentative conversion to protein. *J. Appl. Polym.* **1976**, *20*, 2083–2093. [[CrossRef](#)]
3. Bonn, G.; Concin, R.; Bobleter, O. Hydrothermolysis—A new process for the utilization of biomass. *Wood Sci. Technol.* **1983**, *17*, 195–202. [[CrossRef](#)]
4. Karagöz, S.; Bhaskar, T.; Muto, A.; Sakata, Y.; Oshiki, T.; Kishimoto, T. Low-temperature catalytic hydrothermal treatment of wood biomass: Analysis of liquid products. *Chem. Eng. J.* **2005**, *108*, 127–137. [[CrossRef](#)]
5. Sakaki, T.; Shibata, M.; Miki, T.; Hirose, H.; Hayashi, N. Reaction model of cellulose decomposition in near-critical water and fermentation of products. *Bioresour. Technol.* **1996**, *58*, 197–202. [[CrossRef](#)]
6. Titirici, M.-M.; Antonietti, M. Chemistry and materials options of sustainable carbon materials made by hydrothermal carbonization. *Chem. Soc. Rev.* **2010**, *39*, 103–116. [[CrossRef](#)]
7. Titirici, M.-M.; Thomas, A.; Antonietti, M. Back in the black: Hydrothermal carbonization of plant material as an efficient chemical process to treat the CO<sub>2</sub> problem? *New J. Chem.* **2007**, *31*, 787–789. [[CrossRef](#)]
8. Hu, B.; Wang, K.; Wu, L.; Yu, S.-H.; Antonietti, M.; Titirici, M.-M. Engineering carbon materials from the hydrothermal carbonization process of biomass. *Adv. Mater.* **2010**, *22*, 813–828. [[CrossRef](#)]
9. Titirici, M.-M.; Antonietti, M.; Baccile, N. Hydrothermal carbon from biomass: A comparison of the local structure from poly- to monosaccharides and pentoses/hexoses. *Green Chem.* **2008**, *10*, 1204–1212. [[CrossRef](#)]
10. Demir-Cakan, R.; Baccile, N.; Antonietti, M.; Titirici, M.-M. Carboxylate-rich carbonaceous materials via one-step hydrothermal carbonization of glucose in the presence of acrylic acid. *Chem. Mater.* **2009**, *21*, 484–490. [[CrossRef](#)]
11. Sevilla, M.; Fuertes, A.B. Chemical and structural properties of carbonaceous products obtained by hydrothermal carbonization of saccharides. *Chem. Eur. J.* **2009**, *15*, 4195–4203. [[CrossRef](#)] [[PubMed](#)]

12. Roldán, L.; Santos, I.; Armenise, S.; Fraile, J.M.; García-Bordejé, E. The formation of a hydrothermal carbon coating on graphite microfiber felts for using as structured acid catalyst. *Carbon* **2012**, *50*, 1363–1372. [[CrossRef](#)]
13. Alatalo, S.-M.; Pileidis, F.; Mäkilä, E.; Sevilla, M.; Repo, E.; Salonen, J.; Sillanpää, M.; Titirici, M.-M. Versatile cellulose-based carbon aerogel for the removal of both cationic and anionic metal contaminants from water. *ACS Appl. Mater. Interfaces* **2015**, *7*, 25875–25883. [[CrossRef](#)] [[PubMed](#)]
14. Falco, C.; Baccile, N.; Titirici, M.-M. Morphological and structural differences between glucose, cellulose and lignocellulosic biomass derived hydrothermal carbons. *Green Chem.* **2011**, *13*, 3273–3281. [[CrossRef](#)]
15. Sevilla, M.; Fuertes, A.B. The production of carbon materials by hydrothermal carbonization of cellulose. *Carbon* **2009**, *47*, 2281–2289. [[CrossRef](#)]
16. Tekin, K.; Pileidis, F.D.; Akalin, M.K.; Karagöz, S. Cellulose-derived carbon spheres produced under supercritical ethanol conditions. *Clean Technol. Environ. Policy* **2016**, *18*, 331–338. [[CrossRef](#)]
17. Zhong, R.; Sels, B.F. Sulfonated mesoporous carbon and silica-carbon nanocomposites for biomass conversion. *Appl. Catal. B* **2018**, *236*, 518–545. [[CrossRef](#)]
18. García, J.I.; García-Marín, H.; Pires, E. Glycerol based solvents: Synthesis, properties and applications. *Green Chem.* **2014**, *16*, 1007–1033. [[CrossRef](#)]
19. Sonnati, M.O.; Amigoni, S.; Taffin de Givenchy, E.P.; Darmanin, T.; Choulet, O.; Guittard, F. Glycerol carbonate as a versatile building block for tomorrow: Synthesis, reactivity, properties and applications. *Green Chem.* **2013**, *15*, 283–306. [[CrossRef](#)]
20. García, H.; García, J.I.; Fraile, J.M.; Mayoral, J.A. Solketal: Green and catalytic synthesis and its classification as a solvent. *Chim. Oggi* **2008**, *26*, 10–12.
21. Nanda, M.R.; Zhang, Y.; Yuan, Z.; Qin, W.; Ghaziaskar, H.S.; Xu, C. Catalytic conversion of glycerol for sustainable production of solketal as a fuel additive: A review. *Renew. Sustain. Energy Rev.* **2016**, *56*, 1022–1031. [[CrossRef](#)]
22. De Torres, M.; Jiménez-Osés, G.; Mayoral, J.A.; Pires, E.; De los Santos, M. Glycerol ketals: Synthesis and profits in biodiesel blends. *Fuel* **2012**, *94*, 614–616. [[CrossRef](#)]
23. Nanda, M.R.; Yuan, Z.; Qin, W.; Ghaziaskar, H.S.; Poirier, M.A.; Xu, C. Catalytic conversion of glycerol to oxygenated fuel additive in a continuous flow reactor: Process optimization. *Fuel* **2014**, *128*, 113–119. [[CrossRef](#)]
24. Vicente, G.; Melero, J.A.; Morales, G.; Paniagua, M.; Martín, E. Acetalisation of bio-glycerol with acetone to produce solketal over sulfonic mesostructured silicas. *Green Chem.* **2010**, *12*, 899–907. [[CrossRef](#)]
25. Kowalska-Kus, J.; Held, A.; Frankowski, M.; Nowinska, K. Solketal formation from glycerol and acetone over hierarchical zeolites of different structure as catalysts. *J. Mol. Catal. A* **2017**, *426*, 205–212. [[CrossRef](#)]
26. Li, L.; Korányi, I.; Sels, B.F.; Pescarmona, P. Highly-efficient conversion of glycerol to solketal over heterogeneous Lewis acid catalysts. *Green Chem.* **2012**, *14*, 1611–1619. [[CrossRef](#)]
27. Ricciardi, M.; Falivene, L.; Tabanelli, T.; Proto, A.; Cucciniello, R.; Cavani, F. Bio-Glycidol Conversion to Solketal over Acid Heterogeneous Catalysts: Synthesis and Theoretical Approach. *Catalysts* **2018**, *8*, 391. [[CrossRef](#)]
28. Rodrigues, R.; Gonçalves, M.; Mandelli, D.; Pescarmona, P.P.; Carvalho, W.A. Solvent-free conversion of glycerol to solketal catalysed by activated carbons functionalised with acid groups. *Catal. Sci. Technol.* **2014**, *4*, 2293–2301. [[CrossRef](#)]
29. Gonçalves, M.; Rodrigues, R.; Galhardo, T.S.; Carvalho, W.A. Highly selective acetalization of glycerol with acetone to solketal over acidic carbon-based catalysts from biodiesel waste. *Fuel* **2016**, *181*, 46–54. [[CrossRef](#)]
30. Fraile, J.M.; García-Bordejé, E.; Roldán, L. Deactivation of sulfonated hydrothermal carbons in the presence of alcohols: Evidences for sulfonic esters formation. *J. Catal.* **2012**, *289*, 73–79. [[CrossRef](#)]
31. Fraile, J.M.; García-Bordejé, E.; Pires, E.; Roldán, L. New insights into the strength and accessibility of acid sites of sulfonated hydrothermal carbon. *Carbon* **2014**, *77*, 1157–1167. [[CrossRef](#)]
32. Fraile, J.M.; García-Bordejé, E.; Pires, E. Parametric study of the hydrothermal carbonization of cellulose and effect of acidic conditions. *Carbon* **2017**, *123*, 421–432. [[CrossRef](#)]
33. Lozano-Castelló, D.; Cazorla-Amorós, D.; Linares-Solano, A. Usefulness of CO<sub>2</sub> adsorption at 273 K for the characterization of porous carbons. *Carbon* **2004**, *42*, 1233–1242. [[CrossRef](#)]
34. Urbonaitė, S.; Juárez-Galán, J.M.; Leis, J.; Rodríguez-Reinoso, F.; Svensson, G. Porosity development along the synthesis of carbons from metal carbides. *Microporous Mesoporous Mater.* **2008**, *113*, 14–21. [[CrossRef](#)]

35. Gauden, P.A.; Terzyk, A.P.; Jaroniec, M.; Kowalczyk, P. Bimodal pore size distributions for carbons: Experimental results and computational studies. *J. Colloid Interface Sci.* **2007**, *310*, 205–216. [[CrossRef](#)] [[PubMed](#)]
36. Okpalugo, T.I.T.; Papakonstantinou, P.; Murphy, H.; McLaughlin, J.; Brown, N.M.D. High resolution XPS characterization of chemical functionalised MWCNTs and SWCNTs. *Carbon* **2005**, *43*, 153–161. [[CrossRef](#)]
37. Fraile, J.M.; García-Bordejé, E.; Pires, E.; Roldán, L. Catalytic performance and deactivation of sulfonated hydrothermal carbon in the esterification of fatty acids: Comparison with sulfonic solids of different nature. *J. Catal.* **2015**, *324*, 107–118. [[CrossRef](#)]
38. Margolese, D.; Melero, J.A.; Christiansen, S.C.; Chmelka, B.F.; Stucky, G.D. Direct syntheses of ordered SBA-15 mesoporous silica containing sulfonic acid groups. *Chem. Mater.* **2000**, *12*, 2448–2459. [[CrossRef](#)]
39. Russo, P.A.; Antunes, M.M.; Neves, P.; Wiper, P.V.; Fazio, E.; Neri, F.; Barreca, F.; Mafra, L.; Pillinger, M.; Pinna, N.; et al. Solid acids with SO<sub>3</sub>H groups and tunable surface properties: Versatile catalysts for biomass conversion. *J. Mater. Chem. A* **2014**, *2*, 11813–11824. [[CrossRef](#)]
40. De la Calle, C.; Fraile, J.M.; García-Bordejé, E.; Pires, E.; Roldán, L. Biobased catalyst in biorefinery processes: Sulphonated hydrothermal carbon for glycerol esterification. *Catal. Sci. Technol.* **2015**, *5*, 2897–2903. [[CrossRef](#)]



© 2019 by the authors. Licensee MDPI, Basel, Switzerland. This article is an open access article distributed under the terms and conditions of the Creative Commons Attribution (CC BY) license (<http://creativecommons.org/licenses/by/4.0/>).